IET Control Theory & Applications

Research Article

IET Journals
The Institution of Engineering and Technology

Robust output tracking control of an unmanned aerial vehicle subject to additive state dependent disturbance

ISSN 1751-8644
Received on 21st December 2015
Revised 31st March 2016
Accepted on 18th April 2016
E-First on 14th July 2016
doi: 10.1049/iet-cta.2015.1304
www.ietdl.org

İlker Tanyer[1], Enver Tatlıcıoğlu[1,1] ✉, Erkan Zergeroğlu[2], Meryem Deniz[1], Alper Bayrak[3], Barbaros Özdemirel[1]

[1]*Department of Electrical & Electronics Engineering, İzmir Institute of Technology, Urla, İzmir 35430, Turkey*
[2]*Department of Computer Engineering, Gebze Technical University, Gebze, Kocaeli 41400, Turkey*
[3]*Department of Electrical & Electronics Engineering, Abant İzzet Baysal University, Bolu 14280, Turkey*
✉ *E-mail: envertatlicioglu@iyte.edu.tr*

Abstract: In this study, an asymptotic tracking controller is developed for an aircraft model subject to additive, state-dependent, non-linear disturbance-like terms. Dynamic inversion technique in conjunction with robust integral of the sign of the error term is utilised in the controller design. Compared to the previous studies, the need of acceleration measurements of the aircraft have been removed. In addition, the proposed controller design utilises only the output of aircraft dynamics. Lyapunov based analysis is applied to prove global asymptotic convergence of the tracking error signal. Numerical simulation results are presented to illustrate the performance of the proposed robust controller.

1 Introduction

Obtaining an appropriate model for an unmanned aerial vehicle (UAV) that can be used in the controller design is still an ongoing research and to our best knowledge is a complicated problem. Most of the time, a reliable model is unavailable due to the hard-to-model aerodynamic effects [1]. On top of this, the flight conditions with a slight change can effect the model parameters significantly. External effects such as a gust or gravity can also alter the trajectory of a UAV. From a controller design perspective, the main problem is related to time varying parameters such as the weight of the aircraft which obviously decreases slowly during the flight due to the consumption of fuel. As a result, aside from some very specific cases, the model of a UAV is commonly considered as fully or partially uncertain in controller design. Since model and disturbance uncertainties are inevitable for aircraft models, controller algorithms that require minimum knowledge of system dynamics are preferred for realistic UAV applications.

Among the control design methods commonly applied to aerial vehicles, dynamic inversion is a special type of feedback linearisation control technique [1, 2]. The main idea of dynamic inversion is to transform the non-linear dynamics of the system into a form similar to linear time invariant system via a change of variables [3–11]. Specifically, in [3, 12], dynamic inversion was used for stabilising and tracking problems for aircraft systems. In [4–7], dynamic inversion-based flight control systems were developed for autonomous small-scale helicopters. Dynamic inversion was also utilised in quad-rotor control studies [8–10] and in missile control systems [11]. As can be viewed from the above work when the system dynamics is known dynamic inversion is preferred as uncertainties in system dynamics might result in an increase in the inversion error. To compensate for the possible inversion error, dynamic inversion technique can be fused with robustifying terms as in [13–16]. In [13], a dynamic inversion-based sliding mode control was proposed for attitude tracking control of an aerial vehicle. Yamasaki *et al.* [14] used a robust dynamic inversion controller to maintain high maneuverability and velocity control of a UAV. In [15], a probabilistic robust non-linear control approach fused with dynamic inversion technique was applied to a feedback linearisable aircraft model. In [16], a dynamic inversion controller was combined with a proportional integral controller to linearise a non-linear UAV model and to achieve trajectory tracking. To compensate for uncertainties in the input matrix and additive unstructured disturbance, in [17], MacKunis *et al.* fused the robust controller in [18, 19] with dynamic inversion technique in the design of a robust controller with an adaptive extension. Specifically in [19], asymptotic output tracking was achieved provided a constant estimate of the uncertain input matrix, used in the control design, satisfied some restrictions. However, it was unclear how the estimate would be designed to satisfy the restrictions. Another potential deficit was utilising the time derivative of the output, which includes acceleration information. While acceleration measurements are available for some aircraft systems, utilising them is open to sensor-related issues such as calibration and/or sensor failures.

In this paper [Preliminary results of this paper have appeared in [20].], model reference output tracking control of an aircraft model subject to unstructured uncertainties is discussed. Specifically, the state and the input matrices are considered to be uncertain, and the dynamics is subject to an additive state-dependent non-linear disturbance-like uncertain terms. Furthermore, to remove the need for acceleration measurements, only the output of the aircraft is considered to be available for the controller development. In the design of the controller, a robust integral of the sign of the error component is utilised. Since the input matrix of the aircraft system is considered to be uncertain, a matrix decomposition is also utilised in the development of the error system. The control design is based on Lyapunov-based arguments and analysis techniques. After performing a four-step analysis, global asymptotic stability of the tracking error is ensured. Numerical simulation results which utilised the model of a Obsrey aircraft [21] are then presented to demonstrate the validity of the proposed robust (model-free) controller.

2 Aircraft model

The non-linear aircraft model considered in this work is as follows [1]:

$$\dot{x} = Ax + f(x,t) + Bu, \quad y = Cx \tag{1}$$

where $x(t) \in \mathbb{R}^n$ denotes the state vector, $A \in \mathbb{R}^{n\times n}$ is the constant state matrix, $f(x,t) \in \mathbb{R}^n$ is a state-dependent non-linear disturbance-like term [22] (including gravity, inertial coupling and non-linear gust modeling effects), $B \in \mathbb{R}^{n\times m}$ is the constant input

matrix, $u(t) \in \mathbb{R}^m$ is the control input, $C \in \mathbb{R}^{m\times n}$ is the known output matrix, and $y(t) \in \mathbb{R}^m$ is the output. The number of states is greater than the number of outputs (i.e. $n > m$). The disturbance-like term $f(x,t)$ is considered to be equal to the sum of state-dependent uncertainties, denoted by $f_1(x) \in \mathbb{R}^n$, and time-dependent uncertainties, denoted by $f_2(t) \in \mathbb{R}^n$. The time-dependent uncertainty vector $f_2(t)$ is continuously differentiable and bounded up to its first-order time derivative, and the state-dependent uncertainty vector $f_1(x)$ depends on the state vector $x(t)$ via trigonometric and/or bounded arguments only and thus it is assumed that $f_1(x)$ and $\partial f_1(x)/\partial x$ are bounded for all $x(t)$ (see [21] for the precedence of this type of assumption). When disturbance term, f satisfies the above boundedness assumption and provided the pair (A, B) is controllable, the model in (1) is controllable [23].

3 Control design

In the subsequent development, the system matrices A, B, and the disturbance-like term $f(x,t)$ are considered to be uncertain, and thus, will not be used in the control design. The subsequent control development is derived based on the restriction that only the output $y(t)$ is available.

The main control objective is to ensure that the output of the aircraft, $y(t)$, tracks the output of the following reference model:

$$\dot{x}_m = A_m x_m + B_m u_m, \quad y_m = C x_m \tag{2}$$

where $x_m(t) \in \mathbb{R}^n$ is the reference state vector, $A_m \in \mathbb{R}^{n\times n}$ is the reference state matrix, $B_m \in \mathbb{R}^{n\times m}$ is the reference input matrix, $u_m(t) \in \mathbb{R}^m$ is the reference input, C is the same output matrix in (1), and $y_m(t) \in \mathbb{R}^m$ is the reference output. To ensure the stability of the reference model signals, the reference state matrix A_m is chosen to be Hurwitz, and the reference input $u_m(t)$ and its time derivative are designed as bounded functions of time. Provided these, linear analysis tools can then be utilised to prove that $x_m(t)$, $\dot{x}_m(t)$, $\ddot{x}_m(t)$ and thus, $y_m(t)$, $\dot{y}_m(t)$, $\ddot{y}_m(t)$ are bounded functions of time. Hidden control objective is to ensure that all the signals remain bounded under the closed-loop operation.

To quantify the tracking control objective, an output tracking error, denoted by $e(t) \in \mathbb{R}^m$, is defined as

$$e \triangleq y - y_m. \tag{3}$$

To simplify the presentation of the subsequent analysis, an auxiliary error signal $r(t) \in \mathbb{R}^m$ is introduced as

$$r \triangleq \dot{e} + \Lambda e \tag{4}$$

where $\Lambda \in \mathbb{R}^{m\times m}$ is a constant, positive definite, diagonal control gain matrix. It is noted that since only $y(t)$ is measurable then $\dot{e}(t)$ and thus $r(t)$ are not available, and cannot be utilised in the control design. After substituting (1)–(3) into (4), following expression can be obtained:

$$r = CAx + \Omega u + Cf - CA_m x_m - CB_m u_m + \Lambda e \tag{5}$$

where $\Omega \triangleq CB \in \mathbb{R}^{m\times m}$ is an auxiliary constant matrix. Since B is uncertain, then Ω is uncertain as well. Furthermore, neither symmetry nor positive definiteness of Ω are known. Given these restrictions, the SDU decomposition in [24, 25] is applied to Ω as

$$\Omega = SDU \tag{6}$$

where $S \in \mathbb{R}^{m\times m}$ is a symmetric positive definite matrix, $D \in \mathbb{R}^{m\times m}$ is a diagonal matrix with entries ± 1 and $U \in \mathbb{R}^{m\times m}$ is a unity upper triangular matrix.

The SDU decomposition of Ω for different aircraft models in the literature and for the model in the numerical simulations resulted in the diagonal matrix D being equal to an identity matrix for all these models. However, for the completeness of the presentation, the subsequent controller will be designed to be applicable to any aircraft model without imposing any restrictions on D.

After utilising the SDU decomposition in (6), the time derivative of (5) is obtained as

$$\dot{r} = CA\dot{x} + SDU\dot{u} + C\dot{f} - CA_m\dot{x}_m - CB_m\dot{u}_m + \Lambda\dot{e}. \tag{7}$$

Since S, introduced in (6), is symmetric and positive definite, then so is its inverse, defined as $M \triangleq S^{-1} \in \mathbb{R}^{m\times m}$. Premultiplying (7) with M yields

$$M\dot{r} = N - e + DU\dot{u} \tag{8}$$

where $N(x, \dot{x}, t) \in \mathbb{R}^m$ is defined as

$$N \triangleq M[CA\dot{x} + C\dot{f} - CA_m\dot{x}_m - CB_m\dot{u}_m + \Lambda\dot{e}] + e. \tag{9}$$

The auxiliary vector N can be partitioned as

$$N = N_d + \tilde{N} \tag{10}$$

where $N_d(t) \in \mathbb{R}^m$ contains functions that can be bounded by constants in the sense that

$$|N_{d,i}| \le \zeta_{N_{d,i}} \quad \forall i = 1, ..., m \tag{11}$$

where $N_{d,i}(t) \in \mathbb{R}$ is the ith entry of N_d, $\zeta_{N_{d,i}} \in \mathbb{R}$ are positive bounding constants and $\tilde{N}(x, \dot{x}, e, \dot{e}) \in \mathbb{R}^m$ contains functions that can be bounded by error terms as

$$|\tilde{N}_i| \le \rho_i \left\| z \right\| \quad \forall i = 1, ..., m \tag{12}$$

where $\tilde{N}_i(t) \in \mathbb{R}$ is the ith entry of $\tilde{N}$, $\rho_i \in \mathbb{R}$ are positive bounding constants and $z(t) \in \mathbb{R}^{2m}$ is the combined error defined as

$$z \triangleq \begin{bmatrix} e \\ r \end{bmatrix}. \tag{13}$$

In view of (11) and (12), the entries of the auxiliary vector N can be bounded as

$$|N_i| \le \rho_i \left\| z \right\| + \zeta_{N_{d,i}} \quad \forall i = 1, ..., m. \tag{14}$$

Based on the subsequent stability analysis, the control input is designed as

$$u = -DK[e(t) - e(0) + \Lambda \int_0^t e(\tau)\, \mathrm{d}\tau] - D\Pi \tag{15}$$

where $\Pi(t) \in \mathbb{R}^m$ is an auxiliary filter signal updated according to [Throughout the paper, I_n and $0_{m\times l}$ will be used to represent an $n \times n$ standard identity matrix and an $m \times l$ zero matrix, respectively.]

$$\dot{\Pi}(t) = \beta \mathrm{Sgn}(e(t)) \text{ with } \Pi(0) = 0_{m\times 1} \tag{16}$$

where $\beta \in \mathbb{R}^{m\times m}$ is a constant, positive definite, diagonal control gain matrix, $\mathrm{Sgn}(\cdot)$ denotes the vector sign function, and $K \in \mathbb{R}^{m\times m}$ is a constant, positive definite, diagonal control gain matrix chosen of the form

$$K = I_m + k_g I_m + \mathrm{diag}\{k_{d,1}, k_{d,2}, ..., k_{d,m-1}, 0\} \tag{17}$$

with k_g, $k_{d,1}$,…, $k_{d,m-1} \in \mathbb{R}$ being positive gains. From the structures of (15) and (16), it is easy to see that only the tracking error is required for evaluating the controller. Furthermore, the modelling terms are not required by the controller so it is model-free.

After substituting the time derivative of the control input in (15) into (8), following closed-loop error system is obtained:

$$M\dot{r} = N_d + \tilde{N} - e - DUD\beta \mathrm{Sgn}(e) - D(U - I_m)DKr - Kr \quad (18)$$

where (4), (10) and (16) were utilised.

Since U is unity upper triangular then $U - I_m$ is strictly upper triangular, thus $D(U - I_m)DKr$ term can be written as

$$D(U - I_m)DKr = \left[\Phi^{\mathrm{T}}, 0\right]^{\mathrm{T}} \quad (19)$$

where the entries of $\Phi(r) \in \mathbb{R}^{(m-1)\times 1}$ are defined as

$$\Phi_i = d_i \sum_{j=i+1}^{m} d_j k_j U_{i,j} r_j \text{ for } i = 1, ..., (m-1). \quad (20)$$

Since $d_i = \pm 1 \; \forall i = 1, ..., m$, following upper bound can be obtained for the entries of Φ

$$|\Phi_i| \leq \zeta_{\Phi_i} \| z \| \quad (21)$$

where $\zeta_{U_{i,j}}$ are positive bounding constants satisfying $\zeta_{U_{i,j}} \geq U_{i,j}$ $\forall i, j$. It is important to highlight that ζ_{Φ_i} depends on the control gains k_{i+1},…, k_m.

4 Stability analysis

Theorem 1: The robust controller given in (15) and (16) ensures global asymptotic tracking in the sense that

$$\| z(t) \| \to 0 \text{ as } t \to \infty \quad (22)$$

from its definition in (13), it is clear that $\| e(t) \|, \| r(t) \| \to 0$ as $t \to \infty$ provided that the entries of the control gain matrices K and β are selected by using the following procedure:

i. For $i = m$, β_m is selected according to

$$\beta_m \geq \zeta_{N_{d,m}} \left(1 + \frac{\kappa}{\Lambda_m}\right) \quad (23)$$

and from $i = m - 1$ to $i = 1$, β_i are selected according to

$$\beta_i \geq \left(\zeta_{N_{d,i}} + \sum_{j=i+1}^{m} \zeta_{\Psi_j} \beta_j\right)\left(1 + \frac{\kappa}{\Lambda_i}\right) \quad (24)$$

where $\kappa \in \mathbb{R}$ is some positive bounding constant and the subscript $i = 1, ..., m$ denotes the ith element of the vector or the diagonal matrix.

ii. Control gain k_g is chosen big enough to decrease the constant $\sum_{i=1}^{m} \rho_i^2 / 4k_g$.

iii. Control gains $k_{d,i}$, $i = 1, ..., (m-1)$ are chosen big enough to decrease the constant $\sum_{i=1}^{m-1} \zeta_{\Phi_i^2} / 4k_{d,i}$.

Proof: The proof of theorem consists of four sub-proofs. First, in Appendix 1, boundedness of all the signals under the closed-loop operation will be presented. Second, in Appendix 2, a supporting lemma and its proof is presented. The proof of this lemma provides us to form an upper bound on the terms $\int_0^t |\dot{e}_i(\sigma)| \, \mathrm{d}\sigma$, which will then be utilised in Appendix 3, where the positiveness of an auxiliary integral term will be demonstrated. Finally, in Appendix 4, the asymptotic convergence of the output tracking error is proven. □

The stability analysis mandates the control gains to be chosen to satisfy the procedure detailed in Theorem 1. However, this is a tedious procedure. To address this issue, the self-tuning algorithm in [26, 27] which was designed for similar type of robust controllers are utilised. Specifically, the entries of gain matrices β and K are updated according to

$$\beta_i(t) = \beta_{ci} + |e_i(t)| - |e_i(0)| + \Lambda_i \int_0^t |e_i(\sigma)| \mathrm{d}\sigma \quad (25)$$

$$K_i(t) = k_{ci} + \frac{1}{2} e_i^2(t) - \frac{1}{2} e_i^2(0) + \Lambda_i \int_0^t e_i^2(\sigma) \mathrm{d}\sigma \quad (26)$$

for $i = 1, ..., m$ where β_{ci}, $k_{ci} \in \mathbb{R}$ are positive constant parts of the time-varying gains that can be chosen freely.

5 Numerical simulation results

The model of Osprey fixed wing aerial vehicle in [17, 21], which is a commercially available, low-cost experimental flight testbed, was used in the numerical simulations. Provided the standard assumption that the longitudinal and lateral subsystems of the aircraft are decoupled, the state-space model for the Osprey aircraft testbed can be represented as in (1). The system matrices $A \in \mathbb{R}^{8\times 8}$, $B \in \mathbb{R}^{8\times 4}$ and $C \in \mathbb{R}^{4\times 8}$ are given as

$$A = \begin{bmatrix} A_{\mathrm{lon}} & 0_{4\times 4} \\ 0_{4\times 4} & A_{\mathrm{lat}} \end{bmatrix}, \quad B = \begin{bmatrix} B_{\mathrm{lon}} & 0_{4\times 2} \\ 0_{4\times 2} & B_{\mathrm{lat}} \end{bmatrix}, \quad C = \begin{bmatrix} C_{\mathrm{lon}} & 0_{2\times 4} \\ 0_{2\times 4} & C_{\mathrm{lat}} \end{bmatrix} \quad (27)$$

where A_{lon}, $A_{\mathrm{lat}} \in \mathbb{R}^{4\times 4}$, B_{lon}, $B_{\mathrm{lat}} \in \mathbb{R}^{4\times 2}$, and C_{lon}, $C_{\mathrm{lat}} \in \mathbb{R}^{2\times 4}$ are system matrices for the longitudinal and lateral subsystems. The state vector $x(t) = [x_{\mathrm{lon}}^{\mathrm{T}}, x_{\mathrm{lat}}^{\mathrm{T}}]^{\mathrm{T}} \in \mathbb{R}^8$ where $x_{\mathrm{lon}}(t)$, $x_{\mathrm{lat}}(t) \in \mathbb{R}^4$ denote the longitudinal and lateral state vectors and are defined as

$$x_{\mathrm{lon}} = \begin{bmatrix} v \\ \alpha \\ q \\ \theta \end{bmatrix}, \quad x_{\mathrm{lat}} = \begin{bmatrix} \gamma \\ p \\ \mu \\ \phi \end{bmatrix} \quad (28)$$

where the state variables $v(t)$, $\alpha(t)$, $q(t)$, $\theta(t)$, $\gamma(t)$, $p(t)$, $\mu(t)$, and $\phi(t)$ are velocity, angle of attack, pitch rate, pitch angle, side slip angle, roll rate, yaw rate, and bank angle, respectively.

In the numerical simulations, tracking control of velocity, pitch rate, roll rate, and yaw rate are considered. These four states are controlled by four control inputs. Control inputs are thrust for the forward velocity, aileron for the roll movement, elevator for the pitch movement, and rudder for the yaw movement. The control input $u(t) \triangleq [u_{\mathrm{lon}}^{\mathrm{T}}, u_{\mathrm{lat}}^{\mathrm{T}}]^{\mathrm{T}} \in \mathbb{R}^4$ where $u_{\mathrm{lon}}(t)$, $u_{\mathrm{lat}}(t) \in \mathbb{R}^2$ denote longitudinal and lateral control inputs and are given as

$$u_{\mathrm{lon}} = \begin{bmatrix} u_{\mathrm{e}} \\ u_t \end{bmatrix}, \quad u_{\mathrm{lat}} = \begin{bmatrix} u_{\mathrm{a}} \\ u_{\mathrm{r}} \end{bmatrix} \quad (29)$$

where the control inputs $u_{\mathrm{e}}(t)$, $u_{\mathrm{t}}(t)$, $u_{\mathrm{a}}(t)$, and $u_{\mathrm{r}}(t)$ are elevator deflection angle, control thrust, aileron deflection angle, and rudder deflection angle, respectively.

Following system matrices of the Osprey aircraft, are based on experimentally determined data at a cruising velocity of 25 m/s and at an altitude of 60 m (see (30)) The state-dependent non-linear disturbance-like term $f(x,t) \triangleq [f_{\mathrm{lon}}(x,t)^{\mathrm{T}}, f_{\mathrm{lat}}(x,t)^{\mathrm{T}}]^{\mathrm{T}}$ with $f_{\mathrm{lon}}(x,t)$, $f_{\mathrm{lat}}(x,t) \in \mathbb{R}^4$ being defined as

$$A_{\text{lon}} = \begin{bmatrix} -0.15 & 11.08 & 0.08 & 0 \\ -0.03 & -7.17 & 0.83 & 0 \\ 0 & -37.35 & -9.96 & 0 \\ 0 & 0 & 1 & 0 \end{bmatrix}, \quad A_{\text{lat}} = \begin{bmatrix} -0.69 & -0.03 & -0.99 & 0 \\ -3.13 & -12.92 & 1.1 & 0 \\ 17.03 & -0.10 & -0.97 & 0 \\ 0 & 1 & -0.03 & 0 \end{bmatrix}$$
$$B_{\text{lon}} = \begin{bmatrix} 3 \times 10^{-3} & 0.06 \\ 10^{-5} & 10^{-4} \\ 0.98 & 0 \\ 0 & 0 \end{bmatrix}, \quad B_{\text{lat}} = \begin{bmatrix} 0 & 0 \\ 1.5 & -0.02 \\ -0.09 & 0.17 \\ 0 & 0 \end{bmatrix} \tag{30}$$
$$C_{\text{lon}} = \begin{bmatrix} 0 & 0 & 1 & 0 \\ 1 & 0 & 0 & 0 \end{bmatrix}, \quad C_{\text{lat}} = \begin{bmatrix} 0 & 1 & 0 & 0 \\ 0 & 0 & 1 & 0 \end{bmatrix}.$$

$$A_{\text{lonm}} = \begin{bmatrix} 0.6 & -1.1 & 0 & 0 \\ 2 & -2.2 & 0 & 0 \\ 0 & 0 & -4 & -600 \\ 0 & 0 & 0.1 & -10 \end{bmatrix}, \quad A_{\text{latm}} = \begin{bmatrix} -4 & -600 & 0 & 0 \\ 0.1 & -10 & 0 & 0 \\ 0 & 0 & 0.6 & -1.1 \\ 0 & 0 & 2 & -2.2 \end{bmatrix}$$
$$B_{\text{lonm}} = \begin{bmatrix} 0 & 0.5 \\ 0 & 0 \\ 10 & 0 \\ 0 & 0 \end{bmatrix}, \quad B_{\text{latm}} = \begin{bmatrix} 0 & 0 \\ 10 & 0 \\ 0 & 0.5 \\ 0 & 0 \end{bmatrix}. \tag{33}$$

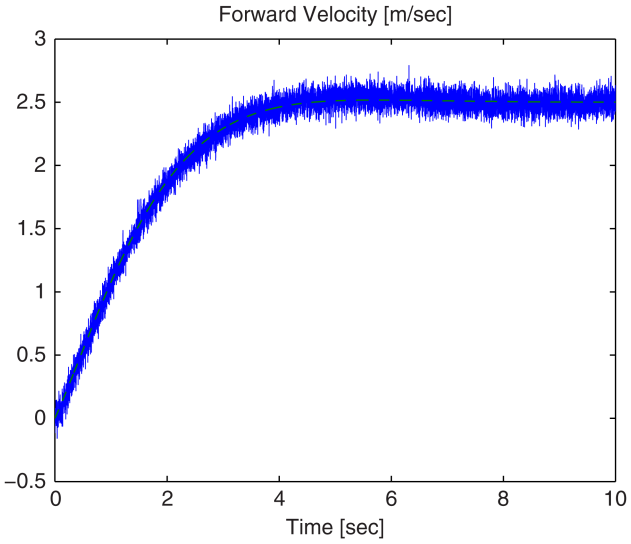

Fig. 1 *Reference forward velocity (dashed line) and the actual forward velocity (solid line)*

$$f_{\text{lon}} \triangleq \begin{bmatrix} -9.81\sin\theta \\ 0 \\ 0 \\ 0 \end{bmatrix} + g(x), \quad f_{\text{lat}} \triangleq \begin{bmatrix} 0.39\sin\phi \\ 0 \\ 0 \\ 0 \end{bmatrix} \tag{31}$$

where $g(x) \in \mathbb{R}^4$ is defined as

$$g \triangleq \frac{1}{V_0}\frac{U_{\text{ds}}}{2}\left[1 - \cos\left(\frac{\pi d_{\text{g}}}{H}\right)\right]\begin{bmatrix} -11.1 \\ 7.2 \\ 37.4 \\ 0 \end{bmatrix} \tag{32}$$

where H denotes the distance along the airplane's flight path for the gust to reach its peak velocity, V_0 is the forward velocity of the aircraft when it enters the gust, $d_{\text{g}} = \int_{t_1}^{t_2} V(t)\,\mathrm{d}t$ represents the distance penetrated into the gust and U_{ds} is the design gust velocity as specified in [22]. Parameter values were chosen as $U_{\text{ds}} = 10.12\,m/s$, H = 15.24 m and V_0 = 25 m/s [21].

Following system matrices were utilised for the reference model: (see (33)) Entries of the reference input $u_m(t) \in \mathbb{R}^4$ are elevator deflection angle, control thrust, aileron deflection angle, and rudder deflection angle, respectively, and was designed as

$$u_m = \begin{bmatrix} 0.2\sin(t) \\ 0.2 \\ 0.2\sin(t) \\ 0.2\sin(t) \end{bmatrix}. \tag{34}$$

The self-tuning algorithm in [26, 27] was used as an add-on and after the algorithm converged, numerical simulations were re-run for the final values of the control gains. Specifically, control gains β and K were obtained from the self-tuning algorithm as

$$\beta = \begin{bmatrix} 72.4 & 0 & 0 & 0 \\ 0 & 81 & 0 & 0 \\ 0 & 0 & 79.6 & 0 \\ 0 & 0 & 0 & 80.8 \end{bmatrix}, \quad K = \begin{bmatrix} 300 & 0 & 0 & 0 \\ 0 & 300.03 & 0 & 0 \\ 0 & 0 & 300 & 0 \\ 0 & 0 & 0 & 300.1 \end{bmatrix} \tag{35}$$

and Λ was chosen as follows:

$$\Lambda = \begin{bmatrix} 2 & 0 & 0 & 0 \\ 0 & 2 & 0 & 0 \\ 0 & 0 & 2 & 0 \\ 0 & 0 & 0 & 2 \end{bmatrix}. \tag{36}$$

In the simulations, the output vector consisted of pitch rate and forward velocity for the longitudinal subsystem, and roll rate and yaw rate for the lateral subsystem. To demonstrate robustness to noise, additive white Gaussian noise with signal-to-noise ratio of 20 dB was added to the velocity measurements. Sampling time was chosen as 0.001 s.

The tracking performance, tracking error and the control inputs are presented in Figs. 1–6, respectively. From Figs. 1–5, it is clear that the tracking objective was satisfied. Control surface limits are given in Table 1 [21]. These limits were determined via the detailed specifications sheet given with the Futaba S3010 standard

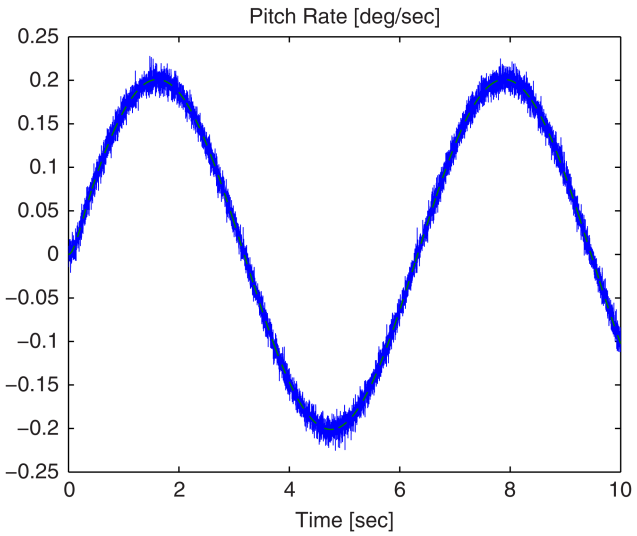

Fig. 2 *Reference pitch rate (dashed line) and the actual pitch rate (solid line)*

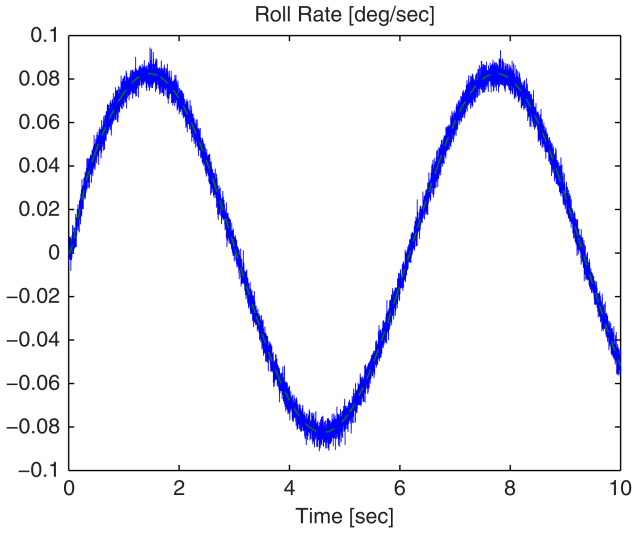

Fig. 3 *Reference roll rate (dashed line) and the actual roll rate (solid line)*

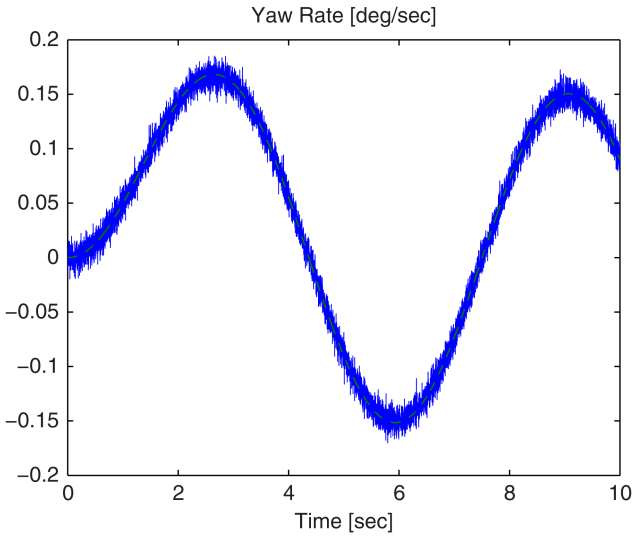

Fig. 4 *Reference yaw rate (dashed line) and the actual yaw rate (solid line)*

ball bearing servo. From Fig. 6 and Table 1, it is clear that the control inputs are in acceptable limits.

In Tables 2 and 3, average maximum steady-state error and average root mean-square error are presented. Five Monte Carlo simulations are performed for different initial state values. Maximum steady-state error is defined as the mean of the last 5 s of the error values. The error values in Tables 2 and 3 show that the proposed controller ensured asymptotic tracking for different initial values of the states.

6 Conclusions

A robust (model-free) controller was designed for an aircraft model subject to unstructured uncertainties in the dynamics and additive state-dependent non-linear disturbance-like terms. In the design of the controller, dynamic inversion technique was used in conjunction with robust integral of the sign of the error terms to compensate for the uncertainties in the dynamic model. Lyapunov type stability analysis techniques were utilised to ensure global asymptotic tracking of the output of a reference model. Numerical simulation results were presented that demonstrate the viability of the proposed methodology.

Table 1 Control input limits used in the simulations

Control thrust saturation limit	± 200 N
Elevator saturation limit	$\pm 30^{\circ}$
Aileron saturation limit	$\pm 30^{\circ}$
Rudder saturation limit	$\pm 30^{\circ}$

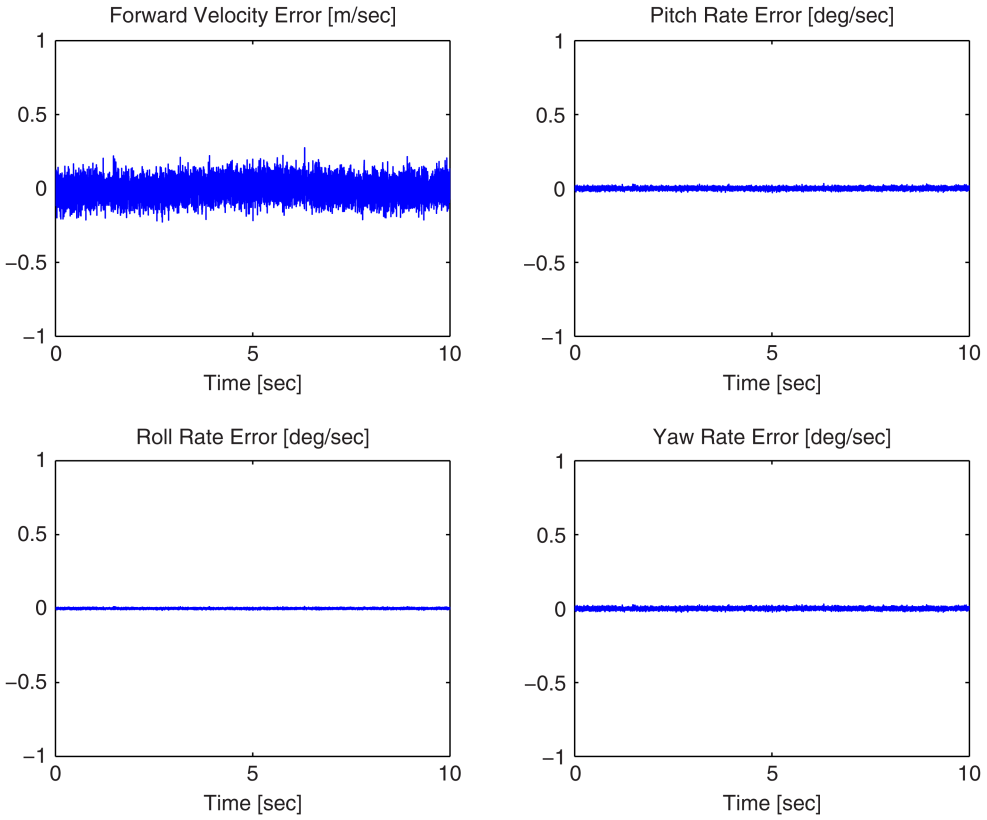

Fig. 5 *Output tracking error* $e(t)$

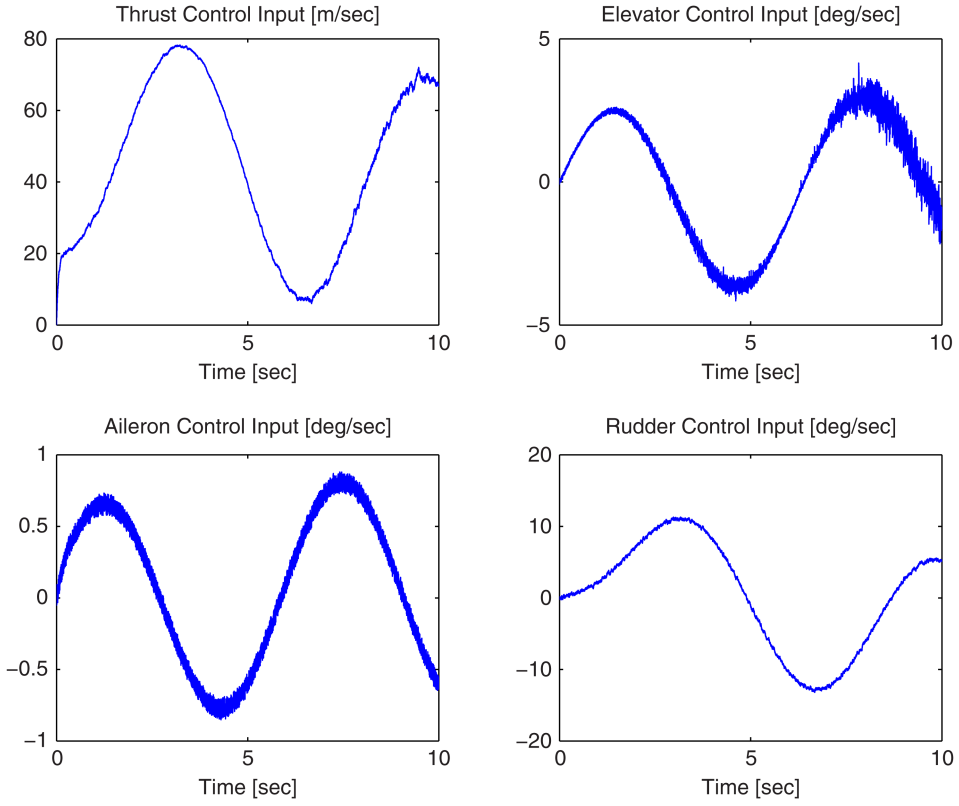

Fig. 6 *Control input* $u(t)$

Table 2 Tabulated steady-state error values for five simulation runs

State	Average maximum steady-state error
forward velocity	0.2751
pitch rate	0.0320
roll rate	0.0132
yaw rate	0.0295

Table 3 Tabulated root mean-square error values for five simulation runs

State	Average root mean-square error
forward velocity	0.0652
pitch rate	0.0078
roll rate	0.0032
yaw rate	0.0072

7 References

[1] Stevens, B.L., Lewis, F.L.: '*Aircraft control and simulation*' (John Wiley & Sons, New York, NY, USA, 2003)

[2] Enns, D., Bugajski, D., Hendrick, R., *et al.*: 'Dynamic inversion: an evolving methodology for flight control design', *Int. J. Control*, 1994, **59**, (1), pp. 71–91

[3] Adams, R.J., Banda, S.S.: 'Robust flight control design using dynamic inversion and structured singular value synthesis', *IEEE Trans. Control Syst. Technol.*, 1993, **1**, (2), pp. 80–92

[4] Zhang, Z., Hu, F., Li, J.: 'Autonomous flight control system designed for small-scale helicopter based on approximate dynamic inversion', Int. Conf. on Advanced Computer Control, Harbin, China, 2011, pp. 185–191

[5] Enns, D., Keviczky, T.: 'Dynamic inversion based flight control for autonomous rmax helicopter', American Control Conf., Minneapolis, MN, USA, 2006, pp. 3916–3923

[6] Cai, G., Cai, A.K., Chen, B.M., *et al.*: 'Construction, modeling and control of a mini autonomous uav helicopter', IEEE Int. Conf. on Automation and Logistics, Qingdao, China, 2008, pp. 449–454

[7] Kemao, P., Miaobo, D., Chen, Ben M., *et al.*: 'Design and implementation of a fully autonomous flight control system for a uav helicopter', Chinese Control Conf., Zhangjiajie, Hunan, China, 2007, pp. 662–667

[8] Das, A., Subbarao, K., Lewis, F.L.: 'Dynamic inversion with zero-dynamics stabilisation for quadrotor control', *IET Control Theory Appl.*, 2009, **3**, (3), pp. 303–314

[9] Al-Hiddabi, S.A.: 'Quadrotor control using feedback linearization with dynamic extension', Int. Symp. on Mechatronics and its Applications, Sharjah, UAE, 2009, pp. 1–3

[10] Lee, B.-Y., Lee, H.-I., Tahk, M.-J.: 'Analysis of adaptive control using on-line neural networks for a quadrotor uav', Int. Conf. on Control, Automation and Systems, Gwangju, Korea, 2013, pp. 1840–1844

[11] Schumacher, C., Khargonekar, P.P.: 'Stability analysis of a missile control system with a dynamic inversion controller', *J. Guidance Control Dyn.*, 1998, **21**, (3), pp. 508–515

[12] Oppenheimer, M.W., Doman, D.: 'Control of an unstable, nonminimum phase hypersonic vehicle model', IEEE Aerospace Conf., Big Sky, MT, USA, 2005, pp. 1–7

[13] Liu, Z., Zhou, F., Zhou, J.: 'Flight control of unpowered flying vehicle based on robust dynamic inversion', Chinese Control Conf., Harbin, China, 2006, pp. 693–698

[14] Yamasaki, T., Sakaida, H., Enomoto, K., *et al.*: 'Robust trajectory-tracking method for uav guidance using proportional navigation', Int. Conf. on Control, Automation and Systems, Seoul, South Korea, 2007, pp. 1404–1409

[15] Wang, Q., Stengel, R.F.: 'Robust nonlinear flight control of a high-performance aircraft', *IEEE Trans. Control Syst. Technol.*, 2005, **13**, (1), pp. 15–26

[16] Xie, Z., Xia, Y., Fu, M.: 'Robust trajectory-tracking method for uav using nonlinear dynamic inversion', Int. Conf. on Cybernetics and Intelligent Systems, Qingdao, China, 2011, pp. 93–98

[17] MacKunis, W., Patre, P.M., Kaiser, M.K., *et al.*: 'Asymptotic tracking for aircraft via robust and adaptive dynamic inversion methods', *IEEE Trans. Control Syst. Technol.*, 2010, **18**, (6), pp. 1448–1456

[18] Xian, B., Dawson, D.M., de Queiroz, M.S., *et al.*: 'A continuous asymptotic tracking control strategy for uncertain nonlinear systems', *IEEE Trans. Autom. Control*, 2004, **49**, (7), pp. 1206–1211

[19] Patre, P.M., MacKunis, W., Makkar, C., *et al.*: 'Asymptotic tracking for systems with structured and unstructured uncertainties', *IEEE Trans. Control Syst. Technol.*, 2008, **16**, (2), pp. 373–379

[20] Tanyer, I., Tatlicioglu, E., Zergeroglu, E.: 'A robust dynamic inversion technique for asymptotic tracking control of an aircraft', Asian Control Conf., Istanbul, Turkey, 2013, pp. 1–6

[21] MacKunis, W.: 'Nonlinear control for systems containing input uncertainty via a Lyapunov-based approach', PhD Dissertation, University of Florida, Gainesville, FL, USA, 2009

[22] Administration, F.A.: 'Federal aviation regulations: airworthiness standards: transport category airplanes', Washington, WA, USA, 2002

[23] Arapostathis, A., George, R.K., Ghosh, M.K.: 'On the controllability of a class of nonlinear stochastic systems', *Syst. Control Lett.*, 2001, **44**, (1), pp. 25–34

[24] Costa, R.R., Hsu, L., Imai, A.K., *et al.*: 'Lyapunov-based adaptive control of mimo systems', *Automatica*, 2003, **39**, (7), pp. 1251–1257

[25] Tao, G.: '*Adaptive control design and analysis*' (John Wiley & Sons, New York, NY, USA, 2003)

[26] Bidikli, B., Tatlicioglu, E., Bayrak, A., *et al.*: 'A new robust integral of sign of error feedback controller with adaptive compensation gain', Int. Conf. on Decision and Control, Florence, Italy, 2013, pp. 3782–3787

[27] Bidikli, B., Tatlicioglu, E., Zergeroglu, E.: 'A self tuning rise controller formulation', American Control Conf., Portland, OR, USA, 2014, pp. 5608–5613

[28] Stepanyan, V., Kurdila, A.: 'Asymptotic tracking of uncertain systems with continuous control using adaptive bounding', *IEEE Trans. Neural Netw.*, 2009, **20**, (8), pp. 1320–1329

[29] Bidikli, B., Tatlicioglu, E., Zergeroglu, E., *et al.*: 'An asymptotically stable continuous robust controller for a class of uncertain mimo nonlinear systems'. 2013, arXiv e-prints:1301.5483

[30] Khalil, H.K., Grizzle, J.: '*Nonlinear systems*' (Prentice-Hall, New York, NY, USA, 2002)

8 Appendix

8.1 Appendix 1: Boundedness proof

In this appendix, boundedness of all the signals under the closed-loop operation will be demonstrated. Let $V_1(z) \in \mathbb{R}$ be a Lyapunov function defined as

$$V_1 \triangleq \frac{1}{2}e^{\mathrm{T}}e + \frac{1}{2}r^{\mathrm{T}}Mr \tag{37}$$

which can be upper and lower bounded as

$$\frac{1}{2}\min\{1, M_{\min}\}\,\|z\|^2 \le V_1 \le \frac{1}{2}\max\{1, M_{\max}\}\,\|z\|^2 \tag{38}$$

where $M_{\min}$ and $M_{\max}$ denote minimum and maximum eigenvalues of M, respectively. After utilising the symmetry of M, time derivative of the Lyapunov function can be written as

$$\dot{V}_1 = e^{\mathrm{T}}\dot{e} + r^{\mathrm{T}}M\dot{r} \tag{39}$$

to which substituting (4), (17)–(19) results in

$$\begin{aligned}\dot{V}_1 = {} & -e^{\mathrm{T}}\Lambda e + r^{\mathrm{T}}N_d + r^{\mathrm{T}}\tilde{N} \\ & -r^{\mathrm{T}}DUD\beta\,\mathrm{Sgn}(e) - r^{\mathrm{T}}\begin{bmatrix}\Phi\\0\end{bmatrix} - r^{\mathrm{T}}r - k_{\mathrm{g}}r^{\mathrm{T}}r - \sum_{i=1}^{m-1}k_{d,i}r_i^2.\end{aligned} \tag{40}$$

Substituting (11), (12), (20) into (40) yields in

$$\begin{aligned}& -e^{\mathrm{T}}\Lambda e + \sum_{i=1}^{m}\zeta_{N_{d,i}}|r_i| + \sum_{i=1}^{m}\rho_i|r_i|\,\|z\| + \zeta_1\|r\| \\ & \quad + \sum_{i=1}^{m-1}\zeta_{\Phi_i}|r_i|\,\|z\| - \|r\|^2 - k_{\mathrm{g}}\|r\|^2 - \sum_{i=1}^{m-1}k\end{aligned} \tag{41}$$

where the upper bound $|r^{\mathrm{T}}DUD\beta\mathrm{Sgn}(e)| \le \zeta_1\|r\|$ with $\zeta_1 \in \mathbb{R}$ being a positive bounding constant was also utilised. After utilising following manipulations:

$$\zeta_1\|r\| + \sum_{i=1}^{m}\zeta_{N_{d,i}}|r_i| \le \frac{1}{2\delta}\|r\|^2 + \delta\left(\zeta_1^2 + \sum_{i=1}^{m}\zeta_{N_{d,i}}^2\right) \tag{42}$$

$$\rho_i|r_i|\,\|z\| - k_{\mathrm{g}}r_i^2 \le \frac{\rho_i^2}{4k_{\mathrm{g}}}\|z\|^2 \tag{43}$$

$$\zeta_{\Phi_i}|r_i|\,\|z\| - k_{d,i}r_i^2 \le \frac{\zeta_{\Phi_i}^2}{4k_{d,i}}\|z\|^2 \tag{44}$$

$\forall i = 1, ..., (m-1)$, where $\delta \in \mathbb{R}$ is a positive damping constant, the right-hand side of (41) can be upper bounded as

$$\dot{V}_1 \leq -\left[\min\left\{\Lambda_{\min}, \left(1 - \frac{1}{2\delta}\right)\right\} - \sum_{i=1}^{m} \frac{\rho_i^2}{4k_g} - \sum_{i=1}^{m-1} \frac{\zeta_{\Phi_i}^2}{4k_{d,i}} \right] \| z \|^2 + \delta\left(\zeta_1^2 + \sum_{i=1}^{m} \zeta_{N_{d,i}}^2\right) \tag{45}$$

where $\Lambda_{\min}$ denotes the minimum eigenvalue of Λ. Provided that the control gains Λ, k_g, $k_{d,1}$,…, $k_{d,m-1}$ are selected sufficiently high, following expression can be obtained for the time derivative of the Lyapunov function:

$$\dot{V}_1 \leq -c_1 V_1 + c_2 \tag{46}$$

where (38) was utilised and c_1 and c_2 are some positive bounding constants defined as

$$\triangleq \frac{2}{\max\{1, M_{\max}\}} \left[\min\left\{\Lambda_{\min}, \left(1 - \frac{1}{2\delta}\right)\right\} - \sum_{i=1}^{m} \frac{\rho_i^2}{4k_g} - \sum_{i=1}^{m-1} \frac{\zeta_\Phi^2}{4k_d} \right] \tag{47}$$

$$c_2 \triangleq \delta\left(\zeta_1^2 + \sum_{i=1}^{m} \zeta_{N_{d,i}}^2\right). \tag{48}$$

From (46), it can be concluded that $V_1(t) \in L_\infty$, and thus, $e(t)$, $r(t) \in L_\infty$. The definition of $r(t)$ in (4) can be utilised to prove that $\dot{e}(t) \in L_\infty$. By using (3) and its time derivative, along with the assumption that the reference model signals being bounded, it can be proven that $y(t)$, $\dot{y}(t)$, $x(t)$, $\dot{x}(t) \in \mathcal{L}_\infty$. The above boundedness statements can be utilised along with (1) to prove that $u(t) \in \mathcal{L}_\infty$. From (15), it is easy to see that $\dot{u}(t) \in \mathcal{L}_\infty$. After utilising the above boundedness statements and the assumption that the reference model signals being bounded along with (7), it is clear that $\dot{r}(t) \in \mathcal{L}_\infty$. Standard signal chasing algorithms can be used to prove that all remaining signals are bounded.

8.2 Appendix 2: Lemma 1 and its proof

Lemma 1: Provided that $e(t)$ and $\dot{e}(t)$ are bounded, the following expression for the upper bound of the integral of the absolute value of the ith entry of $\dot{e}(t)$ can be obtained

$$\int_{t_0}^{t} |\dot{e}_i(\tau)| \, \mathrm{d}\tau \leq \gamma + \kappa \int_{t_0}^{t} |e_i(\tau)| \, \mathrm{d}\tau + |e_i| \tag{49}$$

where γ, $\kappa \in \mathbb{R}$ are some positive bounding constants.

Proof: Since $e(t)$ and $\dot{e}(t)$ are bounded from the above boundedness proof, this lemma can be proven similar to [28]. □

8.3 Appendix 3: Lemma 2 and its proof

Lemma 2: Let the auxiliary function $L(t) \in \mathbb{R}$ be defined as

$$L \triangleq r^{\mathrm{T}}(N_d - DUD\beta \operatorname{Sgn}(e)). \tag{50}$$

If the entries of β are selected to satisfy the conditions in (23) and (24), then it can be concluded that the auxiliary function $P(t) \in \mathbb{R}$ defined as

$$P \triangleq \zeta_b - \int_0^t L(\tau) \, \mathrm{d}\tau \tag{51}$$

is non-negative where $\zeta_b \in \mathbb{R}$ is a positive bounding constant.

Proof: The proof of this lemma is a special case of the proof in [29]. □

8.4 Appendix 4: Asymptotic stability proof

In this appendix, the asymptotic stability of the output tracking error is presented. Let $V_2(w) \in \mathbb{R}$ be a Lyapunov function defined as

$$V_2 \triangleq V_1 + P \tag{52}$$

where $w(t) \triangleq [e^{\mathrm{T}} \quad r^{\mathrm{T}} \quad \sqrt{P}]^{\mathrm{T}} \in \mathbb{R}^{(2m+1)\times 1}$. It should be noted that, the non-negativeness of $P(t)$, which is essential to prove that $V_2(w)$ is a valid Lyapunov function, was proven in Appendix 7.3 [29]. The Lyapunov function in (52) can be upper and lower bounded as follows:

$$\frac{1}{2} \min\{1, M_{\min}\} \| w \|^2 \leq V_2(w) \leq \max\left\{\frac{1}{2} M_{\max}, 1\right\} \| w \|^2 .$$

Taking the time derivative of the Lyapunov function in (52), substituting (40) and the time derivative of (51) and then simplifying results in

$$\dot{V}_2 = -e^{\mathrm{T}}\Lambda e + r^{\mathrm{T}}\tilde{N} - r^{\mathrm{T}}\begin{bmatrix}\Phi \\ 0\end{bmatrix} - r^{\mathrm{T}}r - k_g r^{\mathrm{T}}r - \sum_{i=1}^{m-1} k_{d,i} r_i^2 . \tag{53}$$

After utilising (12) and (21) along with (43) and (44), the right-hand side of (53) can be upper bounded as

$$\dot{V}_2 \leq -\left[\min\{\lambda_{\min}(\Lambda), 1\} - \sum_{i=1}^{m} \frac{\rho_i^2}{4k_g} - \sum_{i=1}^{m-1} \frac{\zeta_{\Phi_i}^2}{4k_{d,i}} \right] \| z \|^2 . \tag{54}$$

Provided that the control gains Λ, k_g, $k_{d,1}$,…, $k_{d,m-1}$ are selected sufficiently high, the below expression can be obtained for the derivative of the Lyapunov function

$$\dot{V}_2 \leq -c_3 \| z \|^2 \tag{55}$$

where c_3 is some positive bounding constant. From (52) and (55), it is clear that $V_2(w)$ is non-increasing and bounded. After integrating (55), it can be concluded that $z(t) \in \mathcal{L}_2$. Since $z(t) \in \mathcal{L}_\infty \cap \mathcal{L}_2$ and $\dot{z}(t) \in \mathcal{L}_\infty$, from Barbalat's lemma [30], $\| z(t) \| \to 0$ as $t \to \infty$, thus meeting the control objective. Since no restrictions with respect to the initial conditions of the error signals were imposed on the control gains, the result is global.